J Therm Anal Calorim (2012) 107:453–461
DOI 10.1007/s10973-011-1430-z

# Synthesis, physical–chemical, and catalytic properties of mixed compositions $Ag/H_3PMo_{12}O_{40}/SiO_2$

**Yu. Trach · V. Sydorchuk · O. Makota · S. Khalameida · R. Leboda · J. Skubiszewska-Zięba · V. Zazhigalov**

Received: 30 December 2010 / Accepted: 23 February 2011 / Published online: 6 March 2011


**Abstract** Deposited catalysts composition $H_3PMo_{12}O_{40}/SiO_2$ and $Ag/H_3PMo_{12}O_{40}/SiO_2$ have been synthesized on the basis of fumed silica, including milling technique. Physical–chemical characteristics of prepared catalysts have been studied by means of XRD, DTA-TG, FTIR, UV–Vis spectroscopy, and adsorption of nitrogen. Catalysts possess meso- or meso-macroporous structure and contain deposited Keggin heteropolycompounds. Deposition of heteropolycompounds on support with high specific surface area results in increase of selectivity to epoxide in epoxidation reactions. The use of milling during catalyst synthesis leads to further growth of selectivity of epoxides formation.

**Keywords** Heteropolycompounds · Milling · X-ray diffraction · Keggin structure · Epoxidation reaction

## Introduction

Heteropolycompounds (HPCs) (polyoxometallates), in particularly heteropolyacids (HPAs), possess combination of attractive properties and advantages owing to their unique Keggin structure. Thus, HPAs contain exceptionally mobile protons, which results in their high acidity and conductivity. Because of this they are promising as acid catalysts, ion exchangers, and solid electrolytes [1–4]. Besides, transition metals with variable valency (V, Mo, and W) are part of the HPCs. Therefore, these compounds are perspective oxidation catalysts [3–5]. In other words, HPCs are versatile materials, particularly bifunctional catalysts.

However, as a rule, specific surface area of HPCs is very low which results in few active sites on their surface. On the other hand, they possess microcrystalline structure. Besides, HPAs are hygroscopic, well soluble in water and oxygen-containing organic solvents, and, as a result, they are chemically unstable for many practical purposes. Therefore, for effective utilization of HPCs in catalytic reactors HPCs should be granular or deposited on granulated supports. It is also possible to incorporate HPCs in structure of matrix-support [6]. This is a proper way to stabilize HPCs. The simplest procedure consists in impregnation of made-ready support by solution of HPAs. Compositions prepared through this technique can be applied as catalysts in gas-phase processes and liquid-phase reactions occurring in the non-polar media. At the same time, one should minimize the loss of useful properties of deposited HPCs and guarantee their accessibility for substrates molecules. In the latter case, incorporated moieties can possess singular physical, chemical, and catalytic properties owing to their nanodispersed state that arise under restrictive influence of pore walls on enlargement of particles (confinement effect) [7]. It should be noted that deposited or incorporated HPCs possess improved properties in comparison with bulk HPCs, and this favors their application in all the above mentioned cases.

Yu. Trach · O. Makota
Institute of Chemistry and Chemical Technologies, L'viv National Polytechnic University, 12 Stepan Bandera Str., Lviv 79013, Ukraine

V. Sydorchuk · S. Khalameida (✉) · V. Zazhigalov
Institute of Sorption and Endoecology, National Academy of Sciences of Ukraine, 13 General Naumov Str., Kyiv 03164, Ukraine
e-mail: svkhal@ukr.net

R. Leboda · J. Skubiszewska-Zięba
Faculty of Chemistry, Maria Curie-Sklodowska University, Maria Curie-Sklodowska Sq. 3, 20-031 Lublin, Poland

It is well known that bulk and supported HPCs are widely applied as catalysts in different oxidation processes [3–5], including homogeneous and heterogeneous epoxidation of some unsaturated compounds [8–10]. In latter case, HPCs display insufficiently high yield of target products, i.e., epoxides. On the other hand, silver-containing, including deposited, catalysts also are effective in numerous epoxidation processes [11, 12].

In this study, a new approach to production of composition Ag/HPA/silica is proposed. It is based on ability of non-porous fumed silica to form structured dispersions (gels) as a result of its mixing with liquids. HPA and water-soluble silver salt are added into reaction mixture on this stage. Besides, prepared wet gels are subjected to milling. Following drying of all wet gels results in formation of porous xerogels. Hence, indicated procedures allow to synthesize Ag/HPCs/silica compositions and to regulate parameters of their chemical, crystal, and porous structure. Catalytic activity of these compositions in the hydroperoxide epoxidation reaction of 1-octene and 1,7-octadiene is also investigated. Therefore, the main goal of this study is to study the influence of synthesis and milling conditions on physical–chemical and catalytic properties of Ag/HPA/silica compositions.

## Experimental

### Reagents

Phosphorous molybdenum acid $H_3PMo_{12}O_{40}\cdot 16H_2O$ (sample A in Table 1) and silver nitrate were obtained from Aldrich. All reagents were analytical grade. Besides, fumed silica-aerosil A300 (Oriana, Ukraine) was utilized as support. 1-Octene, 1,7-octadiene, and chlorbenzene (solvent) were also obtained from Aldrich. *tert*-Butyl hydroperoxide (TBHP) was synthesized from *tert*-butyl alcohol and hydrogen peroxide in the presence of sulfuric acid by the procedure given in [13].

### Synthesis of catalysts

Routine procedure of compositions synthesis was as follows: 1.1 g of $H_3PMo_{12}O_{40}$ was dissolved in 40 mL of water. Then 4.0 g A300 was dispersed in obtained solution under ultrasonic treatment (sample C0 in Table 1). 0.186 or 0.279 g $AgNO_3$ were added to reaction mixture for preparation of two- and three-substituted salt of $H_3PMo_{12}O_{40}$ that corresponds to contain Ag in compositions approximately 2.4 and 3.6% w/w (samples C1, C2, respectively). Duration of both syntheses was 0.5 h. All resulted gels were washed by water and dried during 24 h at 20 °C and for 6 h at 100 °C. Besides, wet gels containing silver before drying subjected to mechanochemical treatment (MChT) (milling) at 400 rpm for 0.5 h (C3, C4). MChT during 45–60 min significantly does not alter structure and properties of catalysts. Milling was carried out using planetary ball mill Pulverisette 7, Premium line (Fritsch Gmbh). The amount of milled mixture (wet gel) was equal to 35 g. 25 Silicon nitride balls with diameter of 10 mm and total mass of 40.5 g and the vessel from silicon nitride with volume of 80 mL were used. Besides, bulk salt composition $Ag_3PMo_{12}O_{40}$ was precipitated in aqueous medium from stoichiometric amounts of $H_3PMo_{12}O_{40}$ and $AgNO_3$ accordingly to procedure described in [14] (sample S).

### Physical–chemical measurements

Crystal structure of prepared samples was examined on diffractometer HZG-4 Carl Zeiss, Jena (Cu $K_\alpha$ radiation). Thermogravimetric analysis was carried out using Derivatograph-C (MOM, Budapest) in air with the heating rate 10 °C $min^{-1}$ in the temperature range 20–800 °C (sample weight—200 mg). The FTIR spectra in the range 4000–450 $cm^{-1}$ were registered using Perkin-Elmer spectrometer "Spectrum-One" (powder-like mixture with KBr, the mass ratio sample/KBr = 1:20). Electron (UV–Vis) spectra of powders were registered on Lambda 35 UV–Vis

**Table 1** Some characteristics prepared compositions

| N n/n | Sample | $S$/$m^2$ $g^{-1}$ | $V_s$/$cm^3$ $g^{-1}$ | $V_\Sigma$/$cm^3$ $g^{-1}$ | $d$/nm | $D$/nm | $\lambda$/nm | Color |
|---|---|---|---|---|---|---|---|---|
| | Pure $SiO_2$ | 282 | 1.56 | 1.58 | 17 | – | – | White |
| 1 | A | 1 | – | – | – | 30 | 500 | Yellow–green |
| 2 | C0 | 214 | 1.15 | 1.16 | 15 | <2 | 466 | Green |
| 3 | C1 | 121 | 0.65 | 1.28 | 27 | 22 | 469 | Green |
| 4 | C2 | 129 | 0.82 | 1.46 | 32 | 24 | 473 | Green |
| 5 | C3 | 162 | 1.01 | 1.03 | 18 | <2 | 482 | Yellow |
| 6 | C4 | 168 | 1.20 | 1.22 | 21 | <2 | 487 | Yellow |
| 7 | S | 2 | – | – | – | 25 | 480 | Orange |

spectrometer (Labsphere RSA-PE-20 diffuse reflectance and transmittance accessory, Perkin-Elmer Instruments).

Parameters of porous structure (specific surface area $S$, sorption pore volume $V_s$, and pore diameter $d$) were determined from isotherms of low-temperature nitrogen adsorption obtained with the help of analyzer ASAP 2405 N ("Micromeritics Instrument Corp"). Outgassing temperature and duration were 150 °C and 2 h, respectively. Total pore volume $V_\Sigma$ was determined via impregnation of samples, dried at 150 °C by liquid water.

### Epoxidation reaction

The epoxidation reaction was carried out in a thermostated glass reactor equipped with a reflux condenser and a magnetic stirrer under an argon atmosphere at temperature 110 °C. Typically, chlorbenzene, TBHP, and 1-octene or 1,7-octadiene were charged into the reactor and heated up to the reaction temperature under stirring and then heteropolycompound catalyst was added. TBHP was used as the oxidant for this reaction to avoid the necessity of application phase transfer catalyst (cocatalyst) which is necessary in the case of hydrogen peroxide. The introduction of the catalyst was considered as the start of the reaction. The reaction mixture was periodically sampled for analysis. The hydroperoxide concentration was determined by iodometric titration. Other components of reaction mixtures were analyzed by using a Hewlett Packard HP 6890 N chromatograph, a capillary column DB-1 packed with dimethylsiloxane. The column temperature was changed from 50 to 250 °C with an increment of 10 °C $min^{-1}$. The rate of TBHP consumption $W_0$ was calculated from the initial linear portion of the kinetic curves.

## Results and discussions

### Structure of deposited samples $H_3PMo_{12}O_{40}/SiO_2$

Composition containing 20% w/w $H_3PMo_{12}O_{40}$ prepared via dispersion A300 into aqueous solution of $H_3PMo_{12}O_{40}$ (sample C0) is X-ray amorphous in accordance with XRD data (diffractogram is not shown). Therefore, deposited HPA phase obviously possesses fine crystalline structure. On the other hand, it can be suggested that these crystallites are weakly aggregated and uniformly distributed at surface of support. The latter may be the result of good solubility of HPA and, consequently, the penetration of the solution to all the pores of the carrier. FTIR findings allow to obtain more detailed information. Thus, spectrum of bulk acid includes the absorption bands (a.b.) which are characteristic for Keggin structure [3, 15]: 1064, 966, 803, and

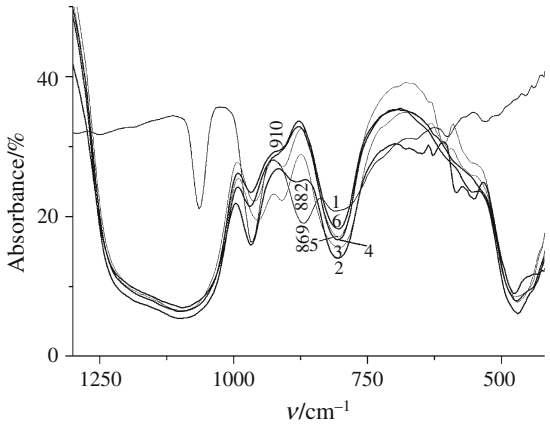


**Fig. 1** FTIR spectra for samples: A (*1*), C0 (*2*), C1 (*3*), C3 (*4*), C2 (*5*), and C4 (*6*)

869 $cm^{-1}$ (Fig. 1, spectrum 1). These a.b. are assigned to the stretching vibrations $\nu_{as}$ P–O, $\nu_{as}$ Mo=O, $\nu_{as}$ Mo–$O_e$–Mo, and $\nu_{as}$ Mo–$O_c$–Mo, respectively. A similar set of a.b. is present on the spectrum of deposited sample C0 (spectrum 2). However, the first three a.b. overlap the a.b. related to silica. The fourth band is shifted toward 882 $cm^{-1}$ (apparently, due to the interaction of acid with the surface of the carrier) and can serve as the only reliable evidence of the maintaining of Keggin structure at surface. Therefore, combination of data obtained by means of XRD and FTIR could indicate high extent of dispersion of $H_3PMo_{12}O_{40}$ on silica surface. Besides, DTA and TG curves of bulk and deposited $H_3PMo_{12}O_{40}$ presented on Figs. 2a, b are similar, which indicates the same thermostability of Keggin structure of both samples: temperature of its decomposition is equal 430–460 °C. The latter data coincide with those described in the study [15].

### Structure of deposited samples $Ag/H_3PMo_{12}O_{40}/SiO_2$

Addition of silver nitrate in reaction mixture results in formation of insoluble two- and three-substituted salts of $H_3PMo_{12}O_{40}$ on silica surface (samples C1, C2, respectively). Comparison of diffractograms 1 and 2 in Fig. 3 demonstrates this. Meantime, crystallite size $D$ of deposited salt calculated in accordance with Sherrer's formula equals about 22–24 nm, while for bulk acid that amounts to 30 nm. At the same time, crystallites of these salts on support surface (as well as those of the bulk $Ag_3PMo_{12}O_{40}$) are strongly aggregated, as evidenced by a sharp decrease in specific surface area of composition $Ag/H_3PMo_{12}O_{40}/SiO_2$ (samples C1, C2) compared with composition $H_3PMo_{12}O_{40}/SiO_2$ (sample C0) (Table 1). This can be explained by the insolubility of these salts. Hence, crystallites of Ag salts on support surface in samples C1 and C2 are distributed non-uniformly.

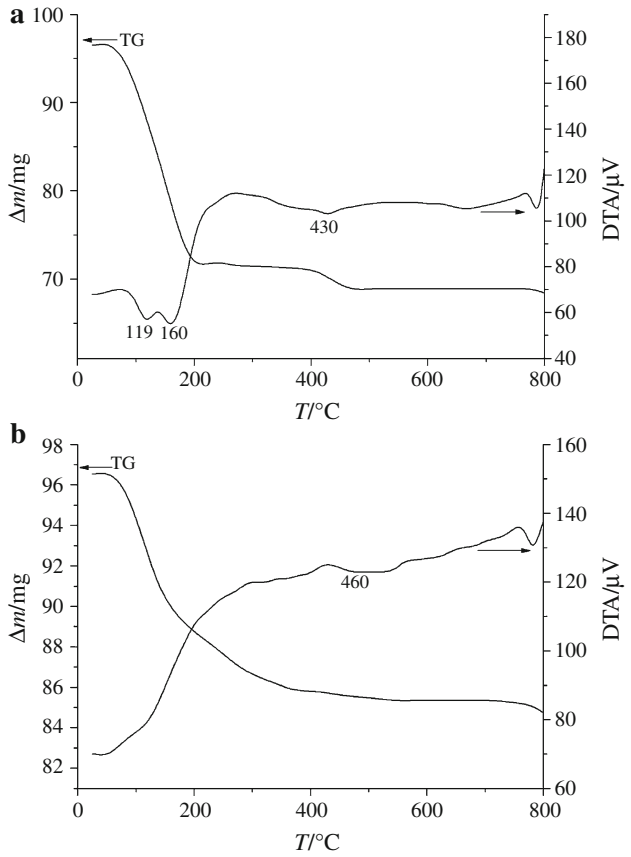


**Fig. 2** DTA–TG curves for bulk $H_3PMo_{12}O_{40}$ (**a**) and $H_3PMo_{12}O_{40}/SiO_2$ (**b**)

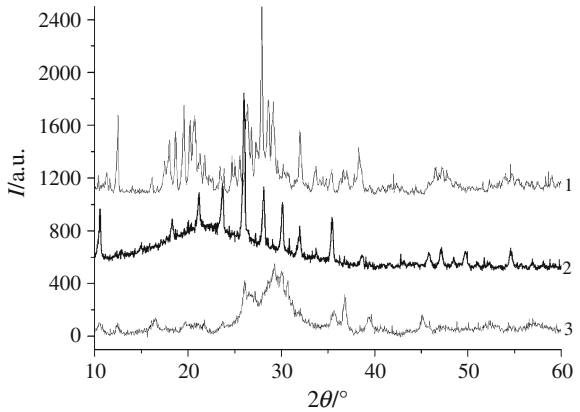


**Fig. 3** XRD for samples: A (*1*), C2 (*2*), and S (*3*)

The FTIR spectra of samples C1 and C2 (Fig. 1, curves 3, 5) contain intensive characteristic band around 910 $cm^{-1}$ that can be assigned to the stretching vibrations $\nu_{as}$ Mo–$O_c$–Mo in heteropolyanion [3]. As mentioned above, this a.b. appears at 869 $cm^{-1}$ for bulk acid (sample A), at 882 $cm^{-1}$ for deposited acid (sample C0), and around 895 $cm^{-1}$ for bulk $Ag_3PMo_{12}O_{40}$ (sample S). Besides, shift of a.b. 933 $cm^{-1}$, that is characteristic for bulk $Ag_3PMo_{12}O_{40}$, to 955–962 $cm^{-1}$ is observed for deposited samples C1 and C2. The latter is also associated with the interaction between deposited phase and support.

## Structure of milled deposited samples $Ag/H_3PMo_{12}O_{40}/SiO_2$

Following milling of both mixtures containing different amount of $AgNO_3$ leads to complete amorphization or dispersing of salt, precipitated on surface, to very fine crystalline state (crystallite size $D$ is lesser than 2 nm, which corresponds to sensitivity of powder XRD). These assumptions can be confirmed by XRD data: no reflection is found on the patterns (these diffractograms are not presented). At the same time, results of FTIR spectroscopy (curves 4, 6) evidence that Keggin structure is only partially destructed: a.b. 910 $cm^{-1}$ as shoulder is present on spectra of these samples (C3, C4), although intensity of this band is lesser than that for unmilled samples (C1, C2). Besides, a.b. around 955–962 $cm^{-1}$ (samples C1, C2) undergoes a shift to 970 $cm^{-1}$ as a result of milling (samples C3, C4). It is possible that the position of this band depends on dispersity of Ag salt: greater shift of this band corresponds to smaller size of crystallites. In other word, formation of Ag salts at silica surface causes reduction of size of their grains, on the one hand and milling of Ag-containing composition leads to further decrease of this parameter, on the other hand. Obviously, molybdenum trioxide appears in system as a result of partial destruction of heteropolyanion although it was not detected by means of used methods of investigations. The increase of specific surface area of milled samples (C3, C4) confirms the latter suggestion.

## UV–Vis spectroscopy study

It is well known that the results obtained with the help of UV–Vis spectroscopy give additional information about properties of bulk and supported HPCs. Thus, absorption edge (and band gap energy) determined from UV–Vis spectra of solid HPCs may serve as a correlating parameter for their oxidation–reduction potential [16, 17]. HPCs are characterized by ability to undergo stepwise, multielectron reversible reactions without structure alteration. UV–Vis spectrum of bulk $H_3PMo_{12}O_{40}$ contains asymmetric broad band with maximum around 415 nm, which is obviously constituted of several components, and peaks at 325 and 215 nm (Fig. 4, curve 1). The latter band can also be a superposition of both transitions of HPA and $Ag^+$, since $Ag^+$ ions also absorb in region 190–230 nm [18]. Indicated broad band (415 nm) is significantly shifted toward lower wavelength for all deposited samples. It also consists of, at least, two components which are centered around 325 and 340–350 nm (curves 2–4). All above mentioned bands are

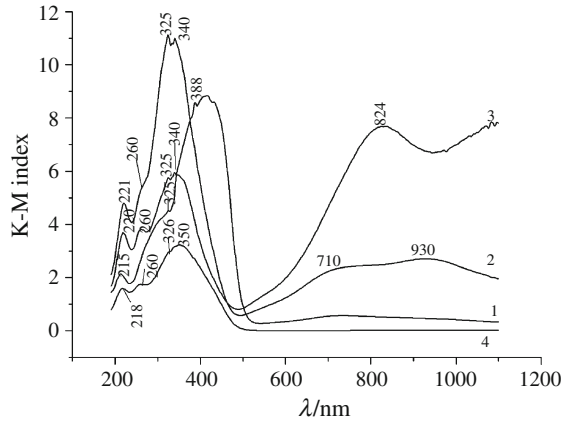


**Fig. 4** UV–Vis spectra for samples: A (*1*), C0 (*2*), C1 (*3*), and C3 (*4*)

attributed to charge transfers (CT) from $O^{2-}$ to $Mo^{6+}$ ions in the Keggin anion [5, 17].

Besides, new low-intensity band at 260 nm is present on spectra of compositions containing Ag (curves 3, 4). This band can be assigned to transitions of $Ag^0$ [12, 18]. The possibility of $Ag^0$ formation is based on the ability of HPCs, including $Mo^{5+}$–$Mo^{6+}$ mixed-valence HPCs, to photocatalytically reduce metal ions in aqueous medium at room temperature [19–21]. The samples C1 and C2 possess dark green color, which can also confirm reduction of part $Ag^+$ to $Ag^0$. However, XRD data do not exhibit existence of crystal silver phase in composition Ag/HPA/silica: the most intensive lines at $2\theta = 38.3$, 44.3, and 64.7°, which are characteristic for metal silver [12], are absent on diffractograms (Fig. 3, curve 2). This can be explained by low content of silver in composition (2.4–3.6% w/w) and incomplete reduction of $Ag^+$ to $Ag^0$ during deposition. It should be noted that UV–Vis spectrum registered for initial HPA (sample A) also contains low-intensive broad band in visible range with maximum around 740 nm (Fig. 4, curve 1). This band, which appears due to intervalence charge-transfer transitions $Mo^{5+} \rightarrow Mo^{6+}$ [5, 17, 22], indicates weak reduced Mo-species in HPA. Increasing of intensity of this band and its shift toward longer wavelength is observed for composition HPA/silica (sample C0). The presence of $Mo^{5+}$ in initial and deposited HPA obviously causes the appearance of zero-valent silver in composition Ag/HPA/silica (samples C1–C4). At the same time, next milling leads to noticeable lowering of intensity of band at 260 nm and change of samples' color to yellow. The latter is the evidence of re-oxidation process $Ag^0 \rightarrow Ag^+$. Besides, the band in visible region disappears from the spectra of milled samples (curve 4). Combination of UV–Vis spectroscopic data allows to suggest that differing ratio $Ag^+/Ag^0$ for initial and milled Ag/HPA/silica compositions is fixed. Particularly, this value increases during milling.

The UV–Vis measurements of studied compositions demonstrate some other features in comparison with bulk HPA. Thus, it is noteworthy that the value of absorption increases in the following series of samples: bulk HPA > deposited HPA > deposited Ag salt > deposited milled Ag salt (curves 2–4). On the other hand, the shift of absorption edge $\lambda$ in UV range (i.e., toward shorter wavelengths) is observed for all deposited samples (Table 1, column 6). In accordance with conclusions of study [17], this means that deposited samples reveal higher oxidation potential. It should be added that similar result was also obtained for $(NH_4)_3PMo_{12}O_{40}/SiO_2$ composition [23].

## Porous structure and specific surface area

During dispersion of aerosil into aqueous solution of $H_3PMo_{12}O_{40}$ or $AgNO_3$ with $H_3PMo_{12}O_{40}$, the formation of porous structure of whole compositions takes place along with the deposition of HPCs on silica surface. Meantime, parameters of porous structure ($S$, $V_\Sigma$, and $d$) depend on the composition of samples and conditions of their following milling, as seen from data presented in Table 1. Thus, mixing of A300 with HPA solution (sample C0) results in formation of xerogel possessing lesser $S$, $V_s$, and $V_\Sigma$ compared with those of pure aerosilogel prepared in the same conditions using water. In this case, last two parameters ($V_s$ and $V_\Sigma$) are equal, which indicates homogeneous mesoporous structure of sample C0; it can be seen from Table 1 and in Fig. 5 (isotherms 1 and 2). Particularly, pore size $d$ (column 5) correspond to the range of mesoporosity. The similar tendency, described also in [6, 15, 23], is the result of the blocking of the smallest pores by moieties. Additional introduction of silver nitrate in reaction mixture, which causes precipitation of Ag salts on silica surface (samples C1 and C2), leads to sharper

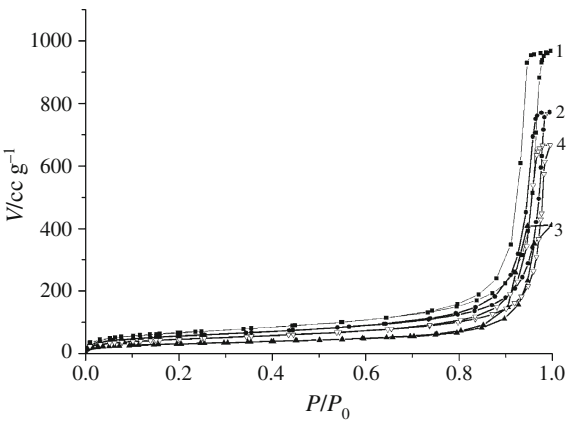


**Fig. 5** Adsorption–desorption isotherms of nitrogen for samples: pure $SiO_2$ (*1*), C0 (*2*), C1 (*3*), and C3 (*4*)

reduction of specific surface area and sorption pore volume $V_s$ of resulted compositions (isotherms 3 on Fig. 5). However, the total pore volume $V_\Sigma$ is much higher than the sorption pore volume $V_s$ (Table 1, column 3). The latter indicates that the samples C1 and C2 contain macropores, which volume amounts to 0.5 $cm^3\ g^{-1}$. In other words, they are the meso-macroporous. The same trend was observed when other insoluble salt, namely ammonium molybdophosphate, was deposited on silica surface [23, 24].

At the same time, following milling causes growth of $S$ and decrease of $V_\Sigma$ (samples C3 and C4 compared with samples C1 and C2, respectively). On the contrary, value of $V_s$ increases and reaches that of the $V_\Sigma$. Consequently, the macropores in the milled samples are not present. The latter can be associated with more dense packing of particles of dispersion during milling. Increasing of $S$ for milled compositions (samples C3, C4) can evidence the supposition, which was formulated above on the basis of XRD findings, about dispersing of Ag salt, precipitated on surface, to very fine crystalline state. Indeed, observed growth of specific surface area may be the result of only dispersion of deposited, Ag salt since milling of pure silica in the same conditions results in decline of its $S$ [25]. If we assume that the observed increase in $S$ of compositions (about 40 $m^2\ g^{-1}$) occurs solely due to dispersion of the deposited salt, then we can calculate the size of grains of salt $D_s$ by the formula: $D_s = (6\rho\ S^{-1}) \times 10^3$ (nm), where $\rho$—density (g $cm^{-3}$).

The resulting value of $D_s$ (approximately 30 nm) is close to the size of crystallites of unmilled compositions (samples C1, C2), calculated from XRD data, and is much smaller grain size of the bulk salt (sample S). Therefore, milling of composition $Ag/H_3PMo_{12}O_{40}/SiO_2$ causes both disaggregation of crystallites of deposited salt and their more uniform distribution on silica surface.

It should also be noted that the shapes of adsorption–desorption isotherms and capillary-condensation hysteresis are identical for all studied samples: pure aerosilogel, $H_3PMo_{12}O_{40}/SiO_2$, and initial and milled $Ag/H_3PMo_{12}O_{40}/SiO_2$. The latter indirectly indicates that the shape of pore of the carrier does not significantly change during the deposition of the active phase and following milling of the compositions.

## Catalytic examination

### *Epoxidation of 1-octene*

The results of the epoxidation reactions of 1-octene and 1,7-octadiene by *tert*-butyl hydroperoxide in the presence of bulk $H_3PMo_{12}O_{40}$ and $Ag_3PMo_{12}O_{40}$ and deposited samples based on HPA and Ag as well as without them are presented in Figs. 6 and 7. The kinetic curves of consumption of TBHP in the studied epoxidation reactions are shown in Figs. 8, 9.

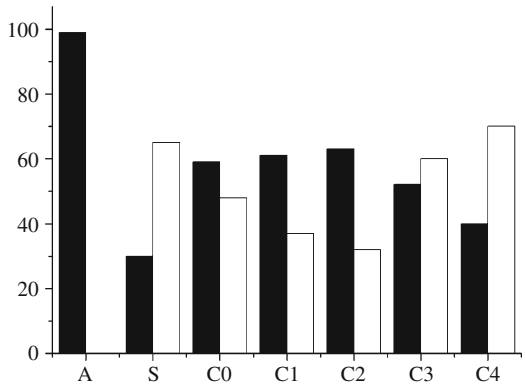


**Fig. 6** Conversion of TBHP (*filled columns*) and selectivity of 1,2-epoxyoctane formation (*open columns*) in the epoxidation reaction of 1-octene by *tert*-butyl hydroperoxide in the presence of the catalysts from Table 1. Reaction conditions: $[1\text{-octene}]_0 = 2$ mol $L^{-1}$, $[TBHP]_0 = 0.4$ mol $L^{-1}$, $[Cat]_0 = 2$ g $L^{-1}$, $T = 383$ K, reaction time = 20 min

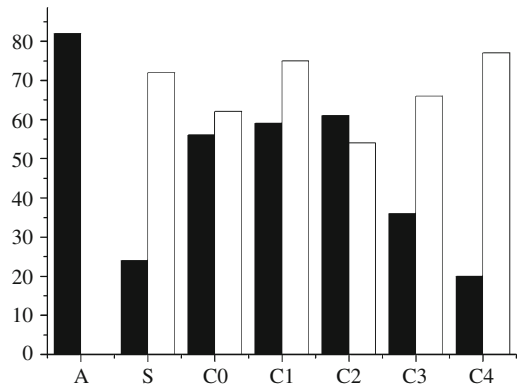


**Fig. 7** Conversion of TBHP (*filled columns*) and selectivity of 1,2-epoxy-7-octene formation (*open columns*) in the epoxidation reaction of 1,7-octadiene by *tert*-butyl hydroperoxide in the presence of the catalysts from Table 1. Reaction conditions: $[1,7\text{-octadiene}]_0 = 2$ mol $L^{-1}$, $[TBHP]_0 = 0.4$ mol $L^{-1}$, $[Cat]_0 = 2$ g $L^{-1}$, $T = 383$ K, reaction time = 20 min

It was established that in the noncatalytic epoxidation reactions of 1-octene and 1,7-octadiene by TBHP *tert*-butyl hydroperoxide is slightly consumed (as can be seen from the kinetic curves), and respective epoxides are not formed in the reaction mixtures.

From Fig. 8 one can see that the introduction of bulk $H_3PMo_{12}O_{40}$ (sample A) in the reaction system significantly affects TBHP conversion in the epoxidation reaction of 1-octene: TBHP is almost completely decomposed during 10 min. However, in the presence of sample A only the process of unproductive decomposition of TBHP takes place, and 1,2-epoxyoctane is not detected in the reaction system TBHP–1-octene (Fig. 6).

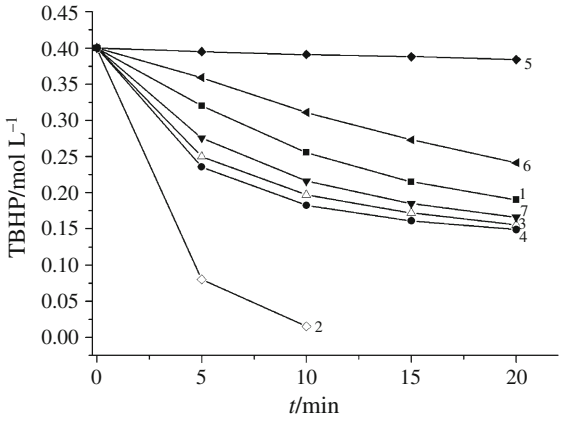


**Fig. 8** Kinetic curves of TBHP consumption in the epoxidation reaction of 1-octene in the presence of catalysts from Table 1

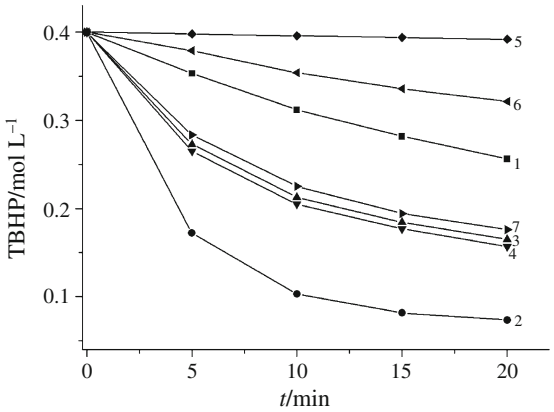


**Fig. 9** Kinetic curves of TBHP consumption in the epoxidation reaction of 1,7-octadiene in the presence of catalysts from Table 1

Bulk salt $Ag_3PMo_{12}O_{40}$ (sample S), on the contrary, displays high selectivity in regard to 1,2-epoxyoctane (65%) and considerably lesser TBHP conversion (30%). Hence, the new deposited samples based on HPA and Ag were further investigated as the catalysts for the epoxidation reactions. It was found that all these prepared compositions catalyze the hydroperoxide epoxidation reaction of 1-octene but their catalytic activity is different (Fig. 6). Thus, deposition of HPA on silica (sample C0) leads to sharp decline of TBHP conversion and similar growth of selectivity of 1,2-epoxyoctane formation. Indicated changes in catalytic performance are obviously caused by uniform distribution of deposited HPA at surface and, consequently, higher accessibility of its active centers for substrate molecules in comparison with that of bulk HPA.

Deposited two- and three-substituted Ag salts (samples C1, C2) reveal slightly higher conversion (61–63%) but appreciably lower selectivity (32–37%). At the same time, milling promotes to sharp (practically twofold in comparison with unmilled compositions) increase of selectivity to 1,2-epoxyoctane (sample C3, C4). On the other hand, TBHP conversion decreases only 1.2–1.5 times. Therefore, the resulted catalytic performance is the best for milled compositions. Thus, deposited HPA and its salts show high TBHP conversion whereas bulk $Ag_3PMo_{12}O_{40}$ displays high selectivity of 1,2-epoxyoctane formation.

*Epoxidation of 1,7-octadiene*

The prepared compositions Ag/HPA/silica as well as bulk $H_3PMo_{12}O_{40}$ and $Ag_3PMo_{12}O_{40}$ were also investigated as the catalysts for the epoxidation of 1,7-octadiene by the same hydroperoxide—TBHP (Figs. 6, 8). All indicated compositions exhibited ability to catalyze this epoxidation reaction. As in the case of 1-octene, the consumption of TBHP without epoxide formation was observed exclusively in the presence of bulk $H_3PMo_{12}O_{40}$. However, the TBHP expenditure was smaller in the epoxidation reaction of 1,7-octadiene (82%) compared with that in the epoxidation reaction of 1-octene (99%). Similar to the epoxidation of 1-octene, in this case deposition of HPA on support resulted in creation of catalyst possessing high selectivity in regard to 1,2-epoxy-7-octene formation (62%). Bulk $Ag_3PMo_{12}O_{40}$ also showed high selectivity (72%) but low TBHP conversion: only 24%. Deposited Ag salts catalysts revealed different properties. Thus, two-substituted salt possesses high value of both TBHP conversion and epoxide selectivity (59 and 75%, respectively). However, its milling worsens the catalytic properties: TBHP conversion and selectivity noticeably decrease. On the contrary, milling of deposited three-substituted salt led to 1.5 time increasing of selectivity and threefold decline of TBHP conversion.

It is interesting to note that the only monoepoxide (1,2-epoxy-7-octene) was product of the epoxidation of 1,7-octadiene by TBHP after 20 min of the reaction time. The prolongation of the reaction time to 1 h did not lead to formation of diepoxide (1,2,7,8-diepoxyoctane).

*Discussion of catalytic results*

Analysis of kinetic curves of TBHP consumption in both epoxidation reactions (Figs. 8, 9, Table 2) permit us to draw some conclusions. It can be seen that TBHP is decomposed with a maximum rate, when non-porous HPA powder (sample A) is a catalyst: rate of TBHP consumption $W_0$ is equal to $4.01 \times 10^{-3}$ and $1.15 \times 10^{-3}$ mol $L^{-1}$ $s^{-1}$ for octene and octadiene, respectively. In the presence of all porous compositions this reaction is accelerated to the lesser degree. However, samples C1 and C2, containing meso- and macro-pores, accelerate the TBHP consumption the most among porous samples ($W_0 = 0.56$–$0.82 \times 10^{-3}$ mol $L^{-1}$ $s^{-1}$). At the same time, milled mesoporous

**Table 2** Values of TBHP consumption rate obtained for different samples in processes of epoxidation

| Substratum | $W \times 10^4$/mol $L^{-1}$ $s^{-1}$ | | | | | | | |
|---|---|---|---|---|---|---|---|---|
| | Without catalyst | A | C0 | C1 | C2 | C3 | C4 | S |
| 1-Octene | 0.18 | 40.01 | 5.63 | 6.81 | 8.22 | 3.03 | 1.30 | 0.81 |
| 1,7-Octadiene | 0.07 | 11.47 | 5.21 | 5.60 | 6.23 | 1.73 | 0.66 | 1.02 |

samples C3, C4 inhibit the consumption of TBHP more than unmilled meso-macroporous samples C1, C2. Sample C0, having smaller mesopores than samples C1 and C2, also destroys the oxidant with a somewhat slower rate. This is obviously the result of the inner-diffusion difficulties arising from the use of porous catalysts. The presence of macropores (the so-called transport pores) in the structure, as observed in the samples C1, C2, somehow eliminates diffusion inhibition.

The changes of catalytic properties, which are observed as a result of deposition of HPA and its salts on silica and next milling, can be associated with alterations in dispersity, surface distribution, and structure of active phase. Thus, deposition of catalyst on support with high specific surface area provides well accessibility of reagents' molecules to active centers of catalyst. $Mo^{6+}$ of polyanion and $Ag^+$ counterion obviously play a role of these centers for studied process. According to the data of XRD, UV–Vis spectroscopy, and adsorption measurements, milling causes following structure changes of deposited phase: (i) increase of its dispersity (specific surface area) that can be seen from Table 1; (ii) more uniform distribution of active phase on support surface, as evidenced by the fact of crystal phase absence; (iii) oxidation of heteropolyanion to fully oxidized state and partial oxidation of $Ag^0$ to $Ag^+$. It is possible that indicated changes facilitate increase of selectivity of epoxides formation. At the same time, some differences in catalytic behavior of $H_3PMo_{12}O_{40}/SiO_2/Ag$ catalysts for 1-octene and 1,2-octadiene epoxidation are not quite understandable.

## Conclusions

Deposition of $H_3PMo_{12}O_{40}$ and its silver salts on silica was carried out by means of dispersion of fine fumed silica into aqueous solutions of $H_3PMo_{12}O_{40}$ and silver nitrate. Resulted compositions contain heteropolyanion possessing Keggin structure with partially reduced molybdenum, which was confirmed with the help of XRD, FTIR, and UV–Vis spectroscopy data. In accordance with UV–Vis spectroscopy, silver is in the form of both $Ag^0$ and $Ag^+$. Next milling results in increase of dispersity of deposited phase that is distributed on surface support more uniformly. Besides, as a result of milling, partial destruction of Keggin structure and reoxidation of $Ag^0$ and molybdenum occur. Prepared compositions possess mesoporous or meso-macroporous (unmilled samples) structure and contain nanodispersed crystallites of $H_3PMo_{12}O_{40}$ or its Ag salts (crystallite size $< 25$ nm) on surface. Indicated structural changes in synthesized compositions result in improved catalytic properties in reaction of epoxidation of unsaturated hydrocarbons. Thus, milled $Ag/H_3PMo_{12}O_{40}/SiO_2$ shows much higher selectivity of epoxides formation in comparison with that of bulk $H_3PMo_{12}O_{40}$ and $Ag_3PMo_{12}O_{40}$ in the system 1-octene (1,2-octadiene)-*tert*-butyl hydroperoxide. This value reaches 70–77% at temperature 110 °C. At the same time, kinetic characteristics of milled samples worsen due to the absence of transport macropores.

## References


1. Pope MT. Heteropoly and isopoly oxometallates. Berlin: Springer; 1983.
2. Heravi MM, Sadjadi S. Recent developments in use of heteropolyacids, their salts and polyoxometalates in organic synthesis. J Iran Chem Soc. 2009;6:1–54.
3. Okuhara T, Mizuno N, Misono M. Catalytic chemistry of heteropoly compounds. Adv Catal. 1996;41:113–252.
4. Moffat JB. The surface and catalytic properties of heteropoly oxometalates, fundamental and applied catalysis. New York: Kluwer Academic/Plenum Publishers; 2001.
5. Cavani F, Mezzogori R, Pigamo A, Trifiro F, Etienne E. Main aspect of the selective oxidation of isobutene to methacrylic acid catalyzed by Keggin-type polyoxometallates. Catal Today. 2001;71:97–110.
6. Sydorchuk V, Zazhigalov V, Khalameida S, Skubiszewska-Zięba J, Charmas B, Leboda R. Deposition of tungsten heteropolycompounds on activated silica surface. Colloids Surf A. 2009;341:53–9.
7. Burt MC, Dave BC. Externally tunable dynamic confinement effect in organosilica sol–gels. J Am Chem Soc. 2006;128:11750–1.
8. Ding Y, Ma B, Gao Q, Li G, Yan L, Suo J. A spectroscopic study on the 12-heteropolyacids of molybdenum and tungsten ($H_3PMo_{12-n}W_n$ $O_{40}$) combined with cetylpiridinium bromide in the epoxidation of cyclopentene. J Mol Catal A. 2005;230:121–8.
9. Casuscelli SG, Crivello ME, Perez CF, Ghione G, Herrero ER, Pizzio LR, Vazquez PG, Caseres CV, Blanco MN. Effect of reaction conditions on limonene epoxidation with $H_2O_2$ catalyzed by supported Keggin heteropolycompounds. Appl Catal A. 2004;274:115–22.
10. Kaczmarczyk E, Janus E, Milchert E. Selective epoxidation of 1,4-bis(allyloxy)butane to 1-allyloxy-glycidoloxybutane in the presence of ionic liquids. J Mol Catal A. 2007;265:148–52.
11. Ted Oyama S., editor. Mechanism in homogeneous and heterogeneous epoxidation catalysis. Amsterdam: Elsevier; 2008.
12. Lu J, Bravo-Suarez JJ, Tabahashi A, Haruta M, Oyama ST. In situ UV–Vis studies of the effect of particle size on the epoxidation of ethylene and propylene on supported silver catalysts with molecular oxygen. J Catal. 2005;232:85–95.

13. Milas NA, Surgenor DM. Studies in organic peroxides. VIII. *t*-butyl hydroperoxide and *di*-t-butyl peroxide. J Am Chem Soc. 1946;68:205–8.
14. Tsignidos GA. Preparation and characterization of 12-molybdophosphoric and molybdosilicic acids and their metal salts. Ind Eng Chem Prod Res Dev. 1974;13:267–74.
15. Popa A, Sasca V, Stefanescu M, Kiš EE, Marinković-Nedučin R. The influence of the nature and textural properties of different supports on the thermal behavior of Keggin type heteropolyacids. J Serb Chem Soc. 2006;71:235–49.
16. Maestre JM, Lopez X, Bo C, Poblet J-M, Casan-Pastor N. Electronic and magnetic properties of α-Keggin anions: a DFT Study of $[XM_{12}O_{40}]^{n-}$, (M = W, Mo; X = $Al^{III}$, $Si^{IV}$, $P^{V}$, $Fe^{III}$, $Co^{II}$, $Co^{III}$) and $[SiM_{11}VO_{40}]^{m-}$ (M = Mo and W). J Am Chem Soc. 2001;123:3749–58.
17. Youn MH, Kim H, Jung JC, Song IK, Barteau KP, Barteau MA. UV–Vis spectroscopy studies of $H_3PMo_{12-x}W_xO_{40}$ heteropolyacid (HPA) catalysts in the solid state: effects of water content and polyatom substitution. J Mol Catal A. 2005;241:227–32.
18. Pestryakov AN, Davydov AA. Study of supported silver states by the method of electron spectroscopy of diffuse reflectance. J Electron Spectrosc Relat Phenom. 1995;74:195–9.
19. Troupis A, Hiskia A, Papaconstantinou E. Photocatalytic reduction-recovery of silver using polyoxometallates. Appl Catal B. 2003;42:305–15.
20. Troupis A, Hiskia A, Papaconstantinou E. Novel synthesis of metal. Nanoparticles by using polyoxometalates as photocatalysts and stabilizers. Ang Chem Int Ed. 2002;41:1911–4.
21. Sharma VK, Yngard RA, Lin E. Silver nanoparticles: green synthesis and their antimicrobical activities. Adv Colloid Interface Sci. 2009;145:83–96.
22. Ballarini N, Candiracci F, Cavani F, Degrand H, Dubois J-L, Lucarelli L, Margotti M, Patinet A, Pigamo A, Trifiro F. The dispersion of Keggin-type P/Mo polyoxmetallates inside silica-gel, and the preparation of catalysts for the oxidation of isobutene to mehacrolein and methacrylic acid. Appl Catal A. 2007;325:263–9.
23. Sydorchuk V, Khalameida S, Skubiszewska-Zięba J, Leboda R. Synthesis and structure of mixed compositions ammonium molybdophosphate/oxide support. J Therm Anal Calorim. 2011;103:257–65.
24. Sasca V, Stefănescu M, Popa A. Thermal behavior of the polyoxometalates derived from $H_3PMo_{12}O_{40}$ and $H_4PVMo_{11}O_{40}$. Influence of some monovalent cations. J Therm Anal Calorim. 2003;72:311–22.
25. Sydorchuk V, Khalameida S, Zazhigalov V, Skubiszewska-Zięba J, Leboda R, Wieczorek-Ciurowa K. Influence of mechanochemical activation in various media on structure of porous and non-porous silicas. Appl Surf Sci. 2010;257:446–50.